Research Square

Preprints are preliminary reports that have not undergone peer review.
They should not be considered conclusive, used to inform clinical practice,
or referenced by the media as validated information.

A Graph-Theoretic Framework for Zika Virus through Vertical Transmission and Stability Analysis.

Renisa P

renisa98pandian@gmail.com

Manonmaniam Sundaranar University

Sujitha S

Manonmaniam Sundaranar University

Angel Jebitha M K

Manonmaniam Sundaranar University

Research Article

Keywords: Zika virus, vertical transmission, newborn babies, microcephaly, basic reproduction number, adjacency matrix, energy, disease-free equilibrium, stability

Posted Date: March 31st, 2026

DOI: https://doi.org/10.21203/rs.3.rs-9221185/v1

License: This work is licensed under a Creative Commons Attribution 4.0 International License.
Read Full License

Additional Declarations: No competing interests reported.

A Graph-Theoretic Framework for Zika Virus through Vertical Transmission and Stability Analysis.

Abstract

The Zika virus, a mosquito-borne pathogen, poses a serious global health threat due to its ability to transmit vertically from infected mothers to newborns, leading to congenital abnormalities and adverse neurological outcomes. A rigorous understanding of vertical transmission dynamics is therefore essential for effective disease prevention and control. In this study, a graph-theoretic framework is proposed to model the human vertical transmission of Zika virus, the birth of babies with microcephaly and asymptomatic infected individuals. The model explicitly incorporates maternal infection states and vertically infected newborn compartments, capturing the mother-to-child transmission pathway. The resulting system is represented as a weighted directed graph, where vertices correspond to epidemiological compartments and directed edges denote transition mechanisms between states. The basic reproduction number R_0 is derived using an energy-based approach applied to the characteristic polynomial associated with the digraph structure, providing an analytical threshold for disease invasion. Furthermore, the Jacobian matrix obtained directly from the digraph at the disease-free equilibrium (DFE) is analyzed to investigate local stability using the Routh–Hurwitz and Gershgorin criteria. The analytical results highlight the critical role of vertical transmission pathways in shaping the overall dynamics of Zika virus spread and underscore the importance of maternal-focused intervention strategies in mitigating congenital Zika outcomes.

Keywords: Zika virus, vertical transmission, newborn babies, microcephaly, basic reproduction number, adjacency matrix, energy, disease-free equilibrium, stability

1 Introduction

The Zika virus (ZIKV), a member of the Spondweni serocomplex of the Flaviviridae family, is a mosquito-borne pathogen primarily transmitted to humans through the bites of infected Aedes mosquitoes. First identified in 1947 from a rhesus macaque in the Zika Forest, ZIKV was long regarded as a cause of mild, self-limiting illness characterized by fever, rash, conjunctivitis, headache, and arthralgia, typically appearing within a few days of infection. For several decades, sporadic cases in Africa and Asia

attracted limited global attention due to the generally benign clinical course observed in most infected individuals.

This perception changed dramatically following large-scale outbreaks in the 21st century, beginning in French Polynesia and later spreading across Latin America [1]. These outbreaks revealed strong epidemiological associations between ZIKV infection and severe neurological complications, including congenital anomalies such as microcephaly and autoimmune disorders such as Guillain–Barré syndrome. In Brazil, thousands of microcephaly cases were reported in the year following ZIKV introduction, far exceeding historical baselines [2]. Subsequent clinical and experimental studies confirmed ZIKV's neurotropism and demonstrated intrauterine infection of the fetal brain, providing a biologically plausible mechanism linking maternal infection, vertical transmission, and congenital Zika syndrome.

ZIKV transmission dynamics are further complicated by multiple infection pathways. While mosquito-borne transmission remains dominant, sexual transmission and a high proportion of asymptomatic infections allow the virus to persist and spread even in the absence of vectors. These features challenge traditional modeling assumptions and highlight the need for refined mathematical frameworks. Early models largely focused on vector transmission alone, whereas more recent studies have incorporated sexual transmission [3], asymptomatic infections [4], and mother-to-child vertical transmission to better assess microcephaly risk and overall disease burden, underscoring the importance of integrated approaches in understanding and controlling ZIKV spread.

In this study, we extend existing approaches by developing a graph-theoretic compartmental model for ZIKV transmission that explicitly incorporates vertical transmission from mother to child, alongside vector-borne routes [5]. The human population is stratified into epidemiologically meaningful classes, including symptomatic and asymptomatic adults and newly born babies, while the mosquito population is similarly structured to reflect infection dynamics. Graph theory provides a natural and powerful framework for representing these interactions: compartments are modeled as vertices, transmission and progression processes as directed edges, and the resulting adjacency matrix encodes the full structure of the system.

Using this graph-based formulation, we derive the basic reproduction number R_0 from the characteristic polynomial of the adjacency matrix evaluated from the derived digraph. Epidemiological dynamics are analyzed using spectral techniques, including graph energy, eigenvalue bounds, and classical criteria such as the Routh–Hurwitz [6] and Gershgorin theorems to analyze stability at the disease-free equilibrium (DFE). This integrated methodology allows us to quantify the relative contributions of vector transmission and vertical transmission to overall epidemic potential, while maintaining biological realism and analytical tractability.

The remaining sections of the paper are organized as follows. Section 2 presents the formulation of the graphical ZIKV model with vertical transmission, defining all compartments, parameters, and the corresponding adjacency matrix. Section 3 derives the basic reproduction number using spectral properties of the graph. Section 4 establishes the main theoretical results, while Section 5 investigates the local stability of

the disease-free equilibrium. Section 6 concludes with a discussion of the epidemiological implications of vertical transmission and asymptomatic infection, and outlines directions for future research and control strategies.

2 Graphical Model

Graphical modeling provides a robust mathematical framework for representing and analyzing complex dynamical systems, making it particularly well-suited for understanding the multifactorial nature of infectious disease transmission. In this context, the proposed graphical model serves as an effective tool for visualizing and quantifying the interactions among key determinants of Zika virus dissemination including vector population dynamics, sexual transmission, vertical transmission, human behavior, environmental factors, and viral persistence.

Among various modeling strategies, compartmental models remain the most widely used because they effectively capture disease progression through transitions between well-defined epidemiological states. The present study introduces a modified compartmental framework inspired by the model proposed by agusto2017. This version explicitly incorporates both vector-to-adult and adult-to-newly born babies (vertical) transmission routes, while sexual transmission is neglected in this model. Subscripts (W), (B) and (V) denote adults,newly born babies and vector populations respectively. The total human population at time t, denoted by $N_H(t)$, is subdivided into two age-structured classes: the newborn (infant) population and the adult population. Each class is further divided into mutually exclusive epidemiological compartments. The newborn population, $N_B(t)$, consists of susceptible newborns $S_B(t)$, exposed newborns $E_B(t)$, asymptomatically infected newborns $A_B(t)$, symptomatically infected newborns without microcephaly $I_B(t)$, symptomatically infected newborns with microcephaly $I_{BM}(t)$, and recovered newborns $R_B(t)$. The adult population, $N_W(t)$, is divided into susceptible adults $S_W(t)$, exposed adults $E_W(t)$, asymptomatically infected adults $A_W(t)$, symptomatically infected adults $I_W(t)$, infected adults with microcephaly $I_{WM}(t)$, and recovered adults $R_W(t)$. The mosquito (vector) population follows an SEI epidemiological structure and is subdivided into susceptible mosquitoes $S_V(t)$, exposed mosquitoes $E_V(t)$, and infectious mosquitoes $I_V(t)$. The total vector population at time t is denoted by $N_V(t)$, which is the sum of these vector compartments. The total population for each group is given as:

$$
\begin{aligned}
N_B(t) &= S_B(t) + E_B(t) + A_B(t) + I_B(t) + I_{BM}(t) + R_B(t), \\
N_W(t) &= S_W(t) + E_W(t) + A_W(t) + I_W(t) + I_{WM}(t) + R_W(t), \\
N_V(t) &= S_V(t) + E_V(t) + I_V(t).
\end{aligned}
$$

All human and mosquito populations are assumed to remain constant over the time scale of the epidemic. The interactions among the human and mosquito compartments are represented using a directed graph defined by [7], $D = (V, E)$, where the vertex set V corresponds to the fifteen epidemiological compartments (twelve human and three vector states), and an edge exists between two vertices whenever a transmission, progression, recovery, maturation, or disease-induced transition occurs at a specified

rate between the corresponding compartments. This graphical formulation forms the basis for constructing the adjacency matrix used in the subsequent analysis.

The digraph $D = (V, E)$ is defined as follows:

$$\begin{aligned} V(D) = \{&S_B(= v_1),\ E_B(= v_2),\ A_B(= v_3),\ I_B(= v_4),\ I_{BM}(= v_5),\ R_B(= v_6),\\ &S_W(= v_7),\ E_W(= v_8),\ A_W(= v_9),\ I_W(= v_{10}),\ I_{\mathrm{WM}}(= v_{11}),\ R_W(= v_{12}),\\ &S_V(= v_{13}),\ E_V(= v_{14}),\ I_V(= v_{15})\}. \end{aligned}$$

$$\begin{aligned} E(D) = \{&(S_B, E_B),\ (E_B, A_B),\ (E_B, I_B),\ (A_B, R_B),\ (I_B, R_B),\\ &(S_W, E_W),\ (E_W, A_W),\ (E_W, I_W),\ (A_W, R_W),\ (I_W, R_W),\\ &(S_V, E_V),\ (E_V, I_V),\ (I_V, S_W),\ (A_W, S_V),\ (I_W, S_V),\\ &(S_B, S_W),\ (E_B, E_W),\ (A_B, A_W),\ (I_B, I_W),\ (R_B, R_W),\ (I_{BM}, I_{WM}),\\ &(R_W, R_B),\ (R_W, I_{BM})\}. \end{aligned}$$

$$\begin{aligned} W(D) = \{&\lambda_B,\ (1-P)\sigma_B,\ P\sigma_B,\ \gamma_B, \lambda_W,\ (1-P)\sigma_W,\ P\sigma_W,\ \gamma_W,\\ &\lambda_V,\ \sigma_V,\ \beta_W b_V,\ \beta_V b_V, \alpha,\ (1-r)q_R\pi_B,\ rq_R\pi_B\} \end{aligned}$$

Each ordered pair $(v_i, v_j) \in E(D)$ represents a directed edge from vertex v_i to vertex v_j in the digraph. The associated weight $w(v_i, v_j) \in W(D)$ denotes the transmission or transition parameter corresponding to that edge.

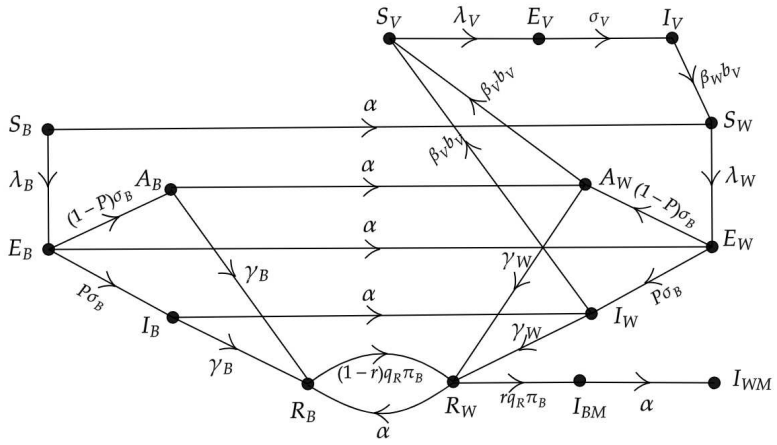


Fig. 1 Graphical representation of vertical transmission of Zika virus

In the Figure 1, vector transmission occurs only between mosquitoes and the adult population. Susceptible adults $S_W(t)$ become exposed $E_W(t)$ after bites from infectious mosquitoes $I_V(t)$. Exposed adults progress to either asymptomatic $A_W(t)$ or symptomatic infectious classes $I_W(t)$, and may further develop microcephaly-related complications $I_{WM}(t)$ or recover $R_W(t)$. Infectious adults transmit the infection back to susceptible mosquitoes $S_V(t)$, which then move to the exposed $E_V(t)$ and infectious $I_V(t)$ stages, completing the vector–adult transmission cycle. Newborns do not acquire infection from mosquitoes due to limited epidemiological evidence and minimal exposure of newborns to mosquito bites.. Instead, infection in newborns occurs only through vertical transmission from infected adults. Consequently, susceptible newborns $S_B(t)$ move to the exposed class $E_B(t)$ due to maternal infection, after which they progress to asymptomatic $A_B(t)$ or symptomatic infectious classes $I_B(t)$, may develop microcephaly $I_{BM}(t)$, and eventually recover $R_B(t)$.

2.1 Range of the model parameters

In the model,the range and baseline values of the parameters are described in Table 1. Baseline values were utilized from [5]. To assess the influence of parameter uncertainty, we analyze the model dynamics over a wide range of parameter values. The force from infection for humans(λ_W, λ_B) are the rates at which infectious individuals infect others and are assumed to be

$$\lambda_W(I_V, N_W) = \frac{\beta_W b_V I_V}{N_W}, \quad \lambda_B(I_V, N_B) = \frac{\eta\beta_B b_V I_V}{N_B},$$

$$\lambda_V(A_W, I_W, N_W) = \beta_V b_V [\frac{I_W + \rho_W A_W}{N_W}]$$

In the force of infection for vectors, the modification parameter associated with infected babies is set to zero ($\eta = 0$) to reflect the biological assumption that infected babies do not contribute to mosquito infection. Hence, only infected adults contribute to vector transmission. Furthermore, based on prior epidemiological data [8], the baseline proportion of infected individuals in the total population is approximated as 0.079, which is used solely for numerical calibration.

2.2 Adjacency Matrix

The adjacency matrix serves as a systematic representation of the interaction network linking humans, mosquitoes, and the infectious agent in studying Zika virus transmission, Through this matrix-based structure, the various transmission routes and infection flows within the population are clearly characterized. A sensitivity analysis is subsequently performed to evaluate how variations in crucial parameters, including transmission rates and vector population levels, influence the basic reproduction number. This threshold quantity, obtained from the dominant eigenvalue of the matrix, reflects how changes in these parameters modify the overall transmission potential of the disease.

Parameter	Description	Range	Baseline
π_B	Birth rate of newly born babies	0.00015-0.00023	0.00018
α	Maturation rate	0.00015-0.00018	0.00017
P	Fraction of asymptomatic adults and newly born babies	$0.1-1$	0.5
$1-P$	Remaining fraction of newly born babies and adults who are infectious	$0.1-1$	0.5
r, q_A, q_I, q_R	Fraction of newborns who are infected and not have microcephaly	$0.1-1$	0.5
$1-r$	Remaining fraction of newly born babies having microcephaly	$0.1-1$	0.5
β_W	Transmission probability(adults)	$0.10-0.75$	0.33
σ_W	Progression rate(adults)	0.0833-0.3333	0.1333
γ_W	Recovery rate(adults)	0.0714-0.3333	0.1176
μ_W	Natural death rate(adults)	0.000036-0.00004	0.000039
β_B	Transmission probability(newborns)	$0.001-0.54$	0.33
σ_B	Progression rate(newborns)	0.0833-0.3333	0.1333
γ_B	Recovery rate(newborns)	0.0714-0.3333	0.1176
μ_B	Natural death rate(newborns)	0.00018-0.00012	0.00014
β_V	Mosquito transmission probability	$0.10-0.75$	0.33
b_V	Mosquito biting rate	$0.33-1.0$	0.5
σ_V	Progression rate(mosquito)	0.1667-0.5	0.2857
μ_V	Natural death rate(mosquito)	0.0238-0.125	0.0476

Table 1 Model parameters, descriptions, ranges, and baseline values used in the simulation.

2.2.1 Definition

The weighted adjacency matrix $A = (a_{ij})$ of a directed graph is defined as

$$a_{ij} = \begin{cases} w(v_i, v_j), & \text{if there exists an edge from } v_i \text{ to } v_j, \\ 0, & \text{otherwise,} \end{cases}$$

where $w(v_i, v_j)$ denotes the weight associated with the edge from vertex v_i to vertex v_j.

Here Figure 1 represents a weighted directed graph (digraph), *D=(V,E)*.Therefore, the adjacency matrix of graph D is as follows,A(D) =

$$\begin{pmatrix}
0 & \lambda_B & 0 & 0 & 0 & 0 & \alpha & 0 & 0 & 0 & 0 & 0 & 0 & 0 & 0 \\
0 & 0 & (1-P)\sigma_B & P\sigma_B & 0 & 0 & 0 & \alpha & 0 & 0 & 0 & 0 & 0 & 0 & 0 \\
0 & 0 & 0 & 0 & \gamma_B & 0 & 0 & 0 & \alpha & 0 & 0 & 0 & 0 & 0 & 0 \\
0 & 0 & 0 & 0 & \gamma_B & 0 & 0 & 0 & 0 & \alpha & 0 & 0 & 0 & 0 & 0 \\
0 & 0 & 0 & 0 & 0 & 0 & 0 & 0 & 0 & 0 & \alpha & 0 & 0 & 0 & 0 \\
0 & 0 & 0 & 0 & 0 & 0 & 0 & 0 & 0 & 0 & 0 & \alpha & 0 & 0 & 0 \\
0 & \lambda_W & 0 & 0 & 0 & 0 & 0 & 0 & 0 & 0 & 0 & 0 & 0 & 0 & 0 \\
0 & 0 & 0 & 0 & 0 & 0 & 0 & 0 & (1-P)\sigma_W & P\sigma_W & 0 & 0 & 0 & 0 & 0 \\
0 & 0 & 0 & 0 & 0 & 0 & 0 & 0 & 0 & 0 & \gamma_W & 0 & \beta_V b_V & 0 & 0 \\
0 & 0 & 0 & 0 & 0 & 0 & 0 & 0 & 0 & 0 & \gamma_W & 0 & \beta_V b_V & 0 & 0 \\
0 & 0 & 0 & 0 & (1-r)q_R\pi_B & rq_R\pi_B & 0 & 0 & 0 & 0 & 0 & 0 & 0 & 0 & 0 \\
0 & 0 & 0 & 0 & 0 & 0 & 0 & 0 & 0 & 0 & 0 & 0 & 0 & 0 & 0 \\
0 & 0 & 0 & 0 & 0 & 0 & 0 & 0 & 0 & 0 & 0 & 0 & 0 & \lambda_V & 0 \\
0 & 0 & 0 & 0 & 0 & 0 & 0 & 0 & 0 & 0 & 0 & 0 & 0 & 0 & \sigma_V \\
0 & 0 & 0 & 0 & 0 & 0 & \beta_W b_V & 0 & 0 & 0 & 0 & 0 & 0 & 0 & 0
\end{pmatrix}$$

The characteristic equation of the above matrix is $\lambda^6(\lambda^9 - B\lambda^7 - A\lambda^2 - AB) = 0$ where $A = \lambda_W\lambda_V\beta_W\beta_V b_V^2\sigma_V\alpha((1-P)\sigma_B + P\sigma_B + (1-P)\sigma_W + P\sigma_W)$ and $B = \alpha(1-r)q_R\pi_B$. The spectrum of the characteristic polynomial consists of six zero eigenvalues, six complex conjugate roots, and three real roots.

3 Energy and Basic Reproduction Number

3.1 Energy of a Digraph

The concept of graph energy was first introduced by Gutman et al.[9], where it was defined as the sum of the absolute values of the eigenvalues of a simple graph [10]. For directed graphs (digraphs), since their adjacency matrices are generally non-symmetric and may have complex eigenvalues, the energy is taken as the sum of the absolute values of the real parts of those eigenvalues. Later, Khan et al.[11] proposed the concept of iota energy for digraphs, defined as the sum of the absolute values of the imaginary parts of their eigenvalues. This idea was further generalized to weighted digraphs by Hafeez and Khan[12]. In the present study, this iota energy framework is utilized to determine the basic reproduction number R_0 of the Zika virus model.

3.1.1 Definition

Let D be a weighted digraph with eigenvalues $\lambda_1, \lambda_2, \ldots, \lambda_n$. Then the energy of D is defined as

$\mathcal{E}(D) = \sum_{k=1}^{n} |Re(\lambda_k)|$, where Re($\lambda_k$) denote the real part of the eigenvalue λ_k.

3.1.2 Definition

Let D be a weighted digraph with eigenvalues $\lambda_1, \lambda_2, \ldots, \lambda_n$, then the iota energy of D is

$\mathcal{E}_c(D) = \sum_{k=1}^{n} |Im(\lambda_k)|$, where $\mathrm{Im}(\lambda_k)$ denote the imaginary part of the eigenvalue λ_k.

3.2 Basic Reproduction Number

In epidemiological modeling, understanding how infectious diseases spread is essential for designing effective control strategies and public health interventions. A central quantity in this analysis is the basic reproduction number, denoted by R_0 [13, 14], which quantifies the potential of a disease to transmit within a population.

3.2.1 Definition

The basic reproduction number, R_0, *represents the expected number of secondary infections generated by a single infectious individual in a wholly susceptible population. It depends on the underlying parameters of the transmission model.*

Once the adjacency matrix of the system is constructed, its eigenvalues are obtained by solving the corresponding characteristic equation. These eigenvalues are then used to compute the basic reproduction number which is defined as

$$R_0 = \mathcal{E}(D) + 2\mathcal{E}_c(D) = \sum_{k=1}^{n} |Re(\lambda_k)| + 2\sum_{k=1}^{n} |Im(\lambda_k)| \tag{1}$$

This formulation allows for determining R_0 directly from the spectral properties of the system matrix, providing insight into disease dynamics. When $R_0 < 1$, each infected individual produces, on average, less than one new case, implying that the infection will gradually disappear. When $R_0 = 1$, the disease remains at a steady state within the population, characterizing an endemic equilibrium. Conversely, if $R_0 > 1$, the infection spreads rapidly, potentially leading to an epidemic unless effective interventions are implemented.

4 Main Results

Theorem 1 *Let* $A = \lambda_W \lambda_V \beta_W \beta_V b_V^2 \sigma_V \alpha\big((1-P)\sigma_B + P\sigma_B + (1-P)\sigma_W + P\sigma_W\big)$, $B = \alpha(1-r)q_R\pi_B$ *and all parameters are nonnegative. Then the basic reproduction number* R_0 *is monotonic increasing in both* A *and* B *defined through the characteristic equation,*

$$\lambda^6(\lambda^9 - B\lambda^7 - A\lambda^2 - AB) = 0.$$

Proof From

$$\lambda^6(\lambda^9 - B\lambda^7 - A\lambda^2 - AB) = 0,$$

Six eigenvalues are zero and do not contribute to R_0. The remaining eigenvalues satisfy $f(\lambda, A, B) = \lambda^9 - B\lambda^7 - A\lambda^2 - AB = 0$.

Case (i): Derivative with respect to A.

Applying the chain rule,

$$\frac{\partial f}{\partial \lambda}\frac{\partial \lambda}{\partial A} + \frac{\partial f}{\partial A} = 0.$$

We get,

$$\frac{\partial f}{\partial A} = -\lambda^2 - B,$$
$$\frac{\partial f}{\partial \lambda} = 9\lambda^8 - 7B\lambda^6 - 2A\lambda.$$

Hence

$$\frac{\partial \lambda}{\partial A} = \frac{\lambda^2 + B}{9\lambda^8 - 7B\lambda^6 - 2A\lambda}.$$

For $A, B \geq 0$, the numerator is nonnegative and the denominator is positive at nonzero eigenvalues. Therefore,

$$\frac{\partial \lambda}{\partial A} \geq 0 \implies \frac{\partial}{\partial A}|\operatorname{Re}(\lambda_k)| \geq 0 \quad \textit{and} \quad \frac{\partial}{\partial A}|\operatorname{Im}(\lambda_k)| \geq 0. \implies \frac{\partial R_0}{\partial A} > 0.$$

Case (ii): Derivative with respect to B.

Similarly,

$$\frac{d}{dB} f(\lambda(A, B), A, B) = \frac{\partial f}{\partial \lambda}\frac{\partial \lambda}{\partial B} + \frac{\partial f}{\partial B} = 0.$$

Since

$$\frac{\partial f}{\partial B} = -\lambda^7 - A,$$

we obtain

$$\frac{\partial \lambda}{\partial B} = \frac{\lambda^7 + A}{9\lambda^8 - 7B\lambda^6 - 2A\lambda}.$$

Again, for $A, B \geq 0$, this quantity is nonnegative. Hence

$$\frac{\partial R_0}{\partial B} > 0.$$

Therefore,

$$\frac{\partial R_0}{\partial A} > 0, \qquad \frac{\partial R_0}{\partial B} > 0$$

and R_0 is monotonic increasing in both A and B.

□

Result 2 *The basic reproduction number $R_0 < 1$ for all lower bounds including baseline parameters and $R_0 > 1$ for all the other upper bounds of the parameters.*

Proof The result follows directly from the numerical analysis in Table 2 and Table 3, since substituting each parameter set into the formula for R_0 yields the stated outcomes. Here the upper bound of r and P are chosen 0.99.

Table 2 Numerical Analysis of A

	λ_W	λ_V	β_W, β_V	b_V	σ_V	α	σ_B, σ_W	P	A
Lower Bound	0.002607	0.00008	0.1	0.33	0.1667	0.00015	0.0833	0.1	9.46152×10^{-16}
Base line	0.013035	0.0177	0.33	0.5	0.2857	0.00017	0.1333	0.5	8.13339×10^{-11}
Upper Bound	0.05925	0.0447	0.75	1	0.5	0.00018	0.3333	0.99	8.93771×10^{-8}

From Table 4, we observe that,

Table 3 Numerical Analysis of B

	$1-r$	q_R	π_B	α	B
Lower Bound	0.01	0.1	0.00015	0.00015	2.25×10^{-11}
Baseline	0.5	0.5	0.00018	0.00017	7.65×10^{-9}
Upper Bound	0.9	1	0.00023	0.00018	3.726×10^{-8}

Table 4 Computation of Basic Reproduction number R_0

	A	B	$\mathcal{E}(D)$	$\mathcal{E}_c(D)$	R_0
Lower Bound	9.46152×10^{-16}	2.25×10^{-11}	0.0321	0.03128246	$0.0947 < 1$
Baseline	8.13339×10^{-11}	7.65×10^{-9}	0.163	0.15856666	$0.480 < 1$
Upper Bound	8.93771×10^{-8}	3.726×10^{-8}	0.443	0.43115552	$1.30 > 1$

(i) For the lower bound parameters, $R_0 = 0.0947 < 1$, implying the disease-free equilibrium is stable and the disease will not sustain transmission and is expected to die out rapidly within the population.
(ii) For the baseline case, $R_0 = 0.48 < 1$, implies that the disease will not sustain transmission and will gradually fade out. Hence, an increase in the baseline parameters (such as Transmission probability per contact to adults and to vectors or biting rate) would push the system to $R_0 \geq 1$, allowing the disease to persist or spread.
(iii) For the upper bound case, $R_0 = 1.30 > 1$, implying that the disease has the potential to persist and slowly spread in the population. □

Corollary 3 *In the characteristic equation,* $\lambda^6(\lambda^9 - B\lambda^7 - A\lambda^2 - AB) = 0$ *where* $A = \lambda_W \lambda_V \beta_W \beta_V b_V^2 \sigma_V \alpha((1-P)\sigma_B + P\sigma_B + (1-P)\sigma_W + P\sigma_W)$ *and* $B = \alpha(1-r)q_R\pi_B$.
(i) If $\sigma_B = \sigma_W = 0$ *or any of the parameters in A such as the mosquito biting rate, the human and Mosquito progression rate etc. becomes zero and* $r = 1$*, then* $A = 0$ *and* $B = 0$*, then the resulting spectrum gives zero energy.*
(ii) If $\mathcal{E}(D) + 2\mathcal{E}_c(D) = 0$*, then the basic reproduction number* $R_0 = 0$ *resulting in the eradication of the disease.*

Proof The characteristic equation is $\lambda^6(\lambda^9 - B\lambda^7 - A\lambda^2 - AB) = 0$. If $r = 1$ i.e the fraction of infected pregnant women who give birth to uninfected babies, then $(1-r) = 0$ gives B=0. Since A is the product of vector parameters, if $\sigma_B = \sigma_W = 0$ or any parameter that gets zero, A equals 0. Also if $\alpha = 0$,then both A and B becomes zero. Thus, if A and B become zero, then the characteristic equation gives zero eigen values yielding the energy of D and the iota energy of D as $\sum_{k=1}^{n} |Re(\lambda_k)| = 0$ and $\sum_{k=1}^{n} |Im(\lambda_k)| = 0$ respectively. We know that the basic reproduction number $R_0 = \mathcal{E}(D) + 2\mathcal{E}_c(D)$. Since the spectrum gives zero energy, the basic reproduction number R_0 becomes zero, indicating the complete absence of the Zika transmission. □

Result 4

(i) If $A = 0$ and $B > 0$, then $R_0 > 0$, and disease transmission occurs purely through vertical transmission.
(ii) If $B = 0$ and $A > 0$, then $R_0 > 0$, and disease transmission occurs purely through vector-mediated (horizontal) transmission.
(iii) If $B > 0$ and $A > 0$, then both horizontal and vertical transmission mechanisms are active.

Proof (i) We know that the characteristic equation of the system is

$$\lambda^6(\lambda^9 - B\lambda^7 - A\lambda^2 - AB) = 0.$$

where $A = \lambda_W\lambda_V\beta_W\beta_V b_V^2\sigma_V\alpha\big((1-P)\sigma_B+P\sigma_B+(1-P)\sigma_W+P\sigma_W\big)$, $B = \alpha(1-r)q_R\pi_B$. If the rate of vector transmission becomes 0, we have only B values. Then the equation becomes

$$\lambda^6\lambda^7(\lambda^2 - B) = 0.$$

which gives two real roots, while the remaining thirteen roots are zero. Thus, the dynamics depend solely on the parameter B, which represents the vertical transmission loop.

$$B = \alpha(1 - r)q_R\pi_B$$

Using Table 3, the lower bound, baseline and the upper bound of B are 2.25×10^{-11}, 7.65×10^{-9} and 3.73×10^{-8} respectively. Then the corresponding R_0 values are 0.00000949, 0.000175 and 0.000386 which are less than zero. Thus in the absence of vector transmission ($A = 0$), vertical transmission alone is insufficient to sustain the infection for the baseline parameter conditions and plays a negligible epidemiological role.

(ii)If the rate of vertical transmission is zero, i.e, if the probability of congenital infection becomes zero we get, $B = 0$. Then the characteristic equation reduces to

$$\lambda^6(\lambda^9 - A\lambda^2) = 0,$$

yielding eight zero roots, one real root, and three pairs of complex conjugate roots. Using Table 2, the lower bound, baseline and the upper bound of A are $9.46 \times 10^{-16}, 8.13 \times 10^{-11}$ and 8.94×10^{-8} and the corresponding R_0 values are 0.0947, 0.4798 and 1.305 respectively. The first two values satisfy $R_0 < 1$, remain below the epidemic threshold. However, the upper bound yields $R_0 = 1.305 > 1$ indicates that the disease spread occurs solely through vector-borne routes, reducing the overall transmission potential and highlighting the critical role of mosquito control in managing the outbreak.

(iii) When $A > 0$ and $B > 0$, the interaction term AB modifies the spectral structure of the system, leading to an increased eigenvalues compared to the individual contributions, yielding the full reproduction number R_0. Thus, the combined transmission pathways amplify the overall epidemic potential. The numerical results indicate that horizontal transmission dominates the epidemic dynamics, while vertical transmission, although weaker in isolation, enhances persistence when coupled with vector-mediated spread. □

5 Local Stability Analysis at the Disease-Free Equilibrium

5.1 Disease-Free Equilibrium (DFE)

Let * denote the equilibrium value of each compartment. In the disease-free equilibrium E_0, all exposed and infectious compartments vanish. Hence,

$$E_B^* = A_B^* = I_B^* = I_{BM}^* = 0, \qquad E_W^* = A_W^* = I_W^* = I_{WM}^* = 0, \qquad E_V^* = I_V^* = 0.$$

Therefore, the susceptible populations satisfy

$$S_B^* = N_B, \qquad S_W^* = N_W, \qquad S_V^* = N_V.$$

Accordingly, the disease-free equilibrium is given by

$$\begin{aligned} E_0 &= (S_B^*, E_B^*, A_B^*, I_B^*, I_{BM}^*, R_B^*, S_W^*, E_W^*, A_W^*, I_W^*, I_{WM}^*, R_W^*, S_V^*, E_V^*, I_V^*) \\ &= (N_B, 0, 0, 0, 0, 0, N_W, 0, 0, 0, 0, 0, N_V, 0, 0). \end{aligned}$$

The stability of this equilibrium determines whether the infection can invade the population.Following the graph-theoretic formulation, the linearized system near the disease-free equilibrium E_0 is governed by the Jacobian matrix. Restricting to the infected subsystem, the Jacobian evaluated at E_0 can be expressed as

$$J(E_0) = F - V,$$

where F represents the rate of appearance of new infections and V denotes the transfer of individuals between infected compartments and their removal due to recovery or death. Rows correspond to destination compartments, and columns correspond to source compartments. Formally, the entries of the new infection matrix $F = (F_{ij})$ are defined as

$$F_{ij} = \begin{cases} a_{ij}, & \text{if the edge } i \leftarrow j \text{ generates new infections,} \\ 0, & \text{otherwise.} \end{cases}$$

$$F = \begin{bmatrix} 0 & 0 & 0 & 0 & 0 & 0 & 0 & 0 & 0 & 0 \\ 0 & 0 & 0 & 0 & 0 & 0 & 0 & 0 & 0 & 0 \\ 0 & 0 & 0 & 0 & 0 & 0 & 0 & 0 & 0 & 0 \\ 0 & 0 & 0 & 0 & 0 & 0 & 0 & 0 & 0 & 0 \\ 0 & 0 & 0 & 0 & 0 & 0 & 0 & 0 & 0 & \beta_W b_V \\ 0 & 0 & 0 & 0 & 0 & 0 & 0 & 0 & 0 & 0 \\ 0 & 0 & 0 & 0 & 0 & 0 & 0 & 0 & 0 & 0 \\ 0 & 0 & 0 & 0 & 0 & 0 & 0 & 0 & 0 & 0 \\ 0 & 0 & 0 & 0 & 0 & \beta_V b_V & \beta_V b_V & 0 & 0 & 0 \\ 0 & 0 & 0 & 0 & 0 & 0 & 0 & 0 & 0 & 0 \end{bmatrix}$$

All remaining edges within the induced infected subgraph those describing movement between exposed and infected states, progression within hosts or vectors, or removal from an infected compartment constitute the transition structure. Diagonal entries of V correspond to the weighted out-degree of each infected-type node, while off-diagonal entries capture the negative of incoming transition weights. The transition matrix is denoted by $V = V_{ij}$ where,

$$V_{ij} = \begin{cases} -a_{ji}, & \text{if } i \leftarrow j \text{ represents progression or removal,} \\ \sum_{k \in X_I} a_{ik}, & \text{if i=j gives the total outflow,} \\ 0, & \text{otherwise.} \end{cases}$$

The digraph used in this study specifies only the transmission relations between compartments but does not explicitly include the natural outflow (death or recovery) of

adult mosquitoes. However, for any epidemiological compartment, a biologically meaningful model requires the presence of at least one outflow mechanism, since infected compartments do not remain indefinitely infectious. For mathematical consistency and according to Agusto et al.[5], natural death rates are included in the disease-free equilibrium for all infected compartments, namely μ_B for baby compartments, μ_W for adult compartments and μ_V for vector compartments. These terms are introduced in the V-matrix to ensure biological realism and invertibility, while preserving the transmission structure defined by the digraph.

$$V = \begin{bmatrix} \sigma_B+\alpha+\mu_B & 0 & 0 & 0 & 0 & 0 & 0 & 0 & 0 & 0 \\ -(1-p)\sigma_B & \gamma_B+\alpha+\mu_B & 0 & 0 & 0 & 0 & 0 & 0 & 0 & 0 \\ -p\sigma_B & 0 & \gamma_B+\alpha+\mu_B & 0 & 0 & 0 & 0 & 0 & 0 & 0 \\ 0 & 0 & 0 & \alpha+\mu_B & 0 & 0 & 0 & 0 & 0 & 0 \\ -\alpha & 0 & 0 & 0 & \sigma_W+\mu_W & 0 & 0 & 0 & 0 & 0 \\ 0 & -\alpha & 0 & 0 & -(1-p)\sigma_W & \gamma_W+\mu_W & 0 & 0 & 0 & 0 \\ 0 & 0 & -\alpha & 0 & -p\sigma_W & 0 & \gamma_W+\mu_W & 0 & 0 & 0 \\ 0 & 0 & 0 & -\alpha & 0 & 0 & 0 & \mu_W & 0 & 0 \\ 0 & 0 & 0 & 0 & 0 & 0 & 0 & 0 & \sigma_V+\mu_V & 0 \\ 0 & 0 & 0 & 0 & 0 & 0 & 0 & 0 & -\sigma_V & \mu_V \end{bmatrix}$$

Theorem 5 (Gershgorin condition for DFE stability) *Let $J(E_0) = F - V$ be the Jacobian matrix of the infected subsystem at the disease-free equilibrium. If the total removal rate in each infected compartment exceeds the corresponding total transmission inflow, namely*

$$\begin{aligned} &\gamma_B+\alpha+\mu_B > (1-p)\sigma_B, \quad && \gamma_W+\mu_W > \alpha+(1-p)\sigma_W, \\ &\gamma_B+\alpha+\mu_B > p\sigma_B, && \gamma_W+\mu_W > \alpha+p\sigma_W, \\ &\sigma_W+\mu_W > \alpha+\beta_W b_V, && \sigma_V+\mu_V > 2\beta_V b_V, \\ &\mu_W > \alpha, && \mu_V > \sigma_V. \end{aligned} \tag{2}$$

then the disease-free equilibrium is locally asymptotically stable and the reproduction energy satisfies $R_0 < 1$.

Proof Let $J = F - V$ denote the Jacobian evaluated at E_0. The diagonal entries of J are negative and represent total removal rates, while off-diagonal entries are nonnegative and represent transmission or transition terms.

For each row i, define the Gershgorin disc

$$D_i = \{z \in \mathbb{C} : |z - J_{ii}| \le r_i\}, \qquad r_i = \sum_{j \neq i} |J_{ij}|.$$

By Gershgorin's circle theorem, every eigenvalue λ of J lies in at least one disc D_i. If $J_{ii} + r_i < 0$ for all i, then each disc lies strictly in the open left half-plane, implying $\Re(\lambda) < 0$ for all eigenvalues. The Gershgorin conditions corresponding to Rows 1 and 4 are trivially satisfied since their off-diagonal entries vanish and all biological parameters are positive. Substituting the explicit diagonal removal rates and transmission radii yields the inequalities in (2). Hence all eigenvalues have negative real parts, and the disease-free equilibrium is locally asymptotically stable. Under these dominance conditions, the associated reproduction energy satisfies $R_0 < 1$. □

Theorem 6 *The disease-free equilibrium point E_0 of the model is locally asymptotically stable if $\mathcal{R}_0 < 1$, where*

$$\mathcal{R}_0^2 = \frac{k_7}{k_4 k_5^2 k_6},$$

and unstable if $\mathcal{R}_0 > 1$.

Proof The Jacobian matrix at the disease-free equilibrium E_0 is a 10×10 matrix. Its characteristic polynomial factorizes as

$$(\lambda + k_1)(\lambda + k_2)^2(\lambda + k_3)(\lambda + \mu_W)\Big(\lambda^5 + C_4\lambda^4 + C_3\lambda^3 + C_2\lambda^2 + C_1\lambda + C_0\Big) = 0.$$

Hence five eigenvalues are $-k_1$, $-k_2$, $-k_3$, $-k_2$, $-\mu_W$. Since all parameters k_i and μ_W are positive, these five eigenvalues are strictly negative. Therefore stability of E_0 depends only on the roots of the fifth-degree polynomial

$$\lambda^5 C_5 + \lambda^4 C_4 + \lambda^3 C_3 + \lambda^2 C_2 + \lambda C_1 + C_0 = 0,$$

where

$$\begin{aligned}
C_5 &= 1,\\
C_4 &= k_6 + 2k_5 + k_4 + \mu_V,\\
C_3 &= 2k_6k_5 + k_5^2 + k_4k_6 + 2k_4k_5 + k_6\mu_V + 2k_5\mu_V + k_4\mu_V,\\
C_2 &= k_5^2k_6 + 2k_4k_5k_6 + k_4k_5^2 + 2k_6k_5\mu_V + k_5^2\mu_V + k_4k_6\mu_V + 2k_4k_5\mu_V,\\
C_1 &= k_4k_5^2\mu_V + 2k_4k_5k_6\mu_V + k_5^2k_6\mu_V + k_4k_5^2k_6 - k_7,\\
C_0 &= k_4k_6k_5^2\mu_V - k_5k_7.
\end{aligned}$$

with

$$\begin{gathered}
k_1 = \sigma_B + \mu_B + \alpha, \quad k_2 = \gamma_B + \mu_B + \alpha, \quad k_3 = \mu_B + \alpha,\\
k_4 = \sigma_W + \mu_W, \quad k_5 = \gamma_W + \mu_W, \quad k_6 = \sigma_V + \mu_V,\\
k_7 = \sigma_W\sigma_V\beta_W\beta_V b_V^2.
\end{gathered}$$

Since all epidemiological parameters are strictly positive, it follows immediately that $C_5 > 0, \quad C_4 > 0, \quad C_3 > 0, \quad C_2 > 0$. Hence the sign of the remaining coefficients C_1 and C_0 determines the stability behaviour.
For a fifth–degree polynomial $a_5\lambda^5 + a_4\lambda^4 + a_3\lambda^3 + a_2\lambda^2 + a_1\lambda + a_0 = 0$ all roots have negative real parts if and only if

$$T_0, T_1, T_2, T_3, T_4, T_5 > 0,$$

where

$$T_0 = a_5, \qquad T_1 = a_4,$$

$$T_2 = \begin{vmatrix} a_4 & a_5 \\ a_2 & a_3 \end{vmatrix}, \qquad T_3 = \begin{vmatrix} a_4 & a_5 & 0 \\ a_2 & a_3 & a_4 \\ a_0 & a_1 & a_2 \end{vmatrix}.$$

By the Liénard–Chipart test, it is sufficient to show that $C_5, C_4, C_3, C_2, C_1, C_0 > 0$ and that the even Hurwitz determinants T_0, T_2, T_4 are positive. From the expression of C_1, $C_1 > 0$ iff $k_7 < k_4k_5^2k_6$. Similarly, $C_0 > 0$ iff $k_5k_7 < k_4k_6k_5^2\mu_V$. Dividing the second inequality by $k_5 > 0$, we obtain $k_7 < k_4k_5k_6\mu_V$.

Define

$$\mathcal{R}_0^2 = \frac{k_7}{k_4k_5^2k_6}.$$

Then $\mathcal{R}_0 < 1$ implies $k_7 < k_4 k_5^2 k_6$, which guarantees $C_1 > 0$. Since $\mu_V > 0$, it also ensures $C_0 > 0$. Thus for $\mathcal{R}_0 < 1, C_i > 0 \quad$ for all $i = 0, 1, \ldots, 5$.
We now show that the even-numbered T_k are positive for $\mathcal{R}_0 < 1$. First, $T_0 = C_5 = 1 > 0$. Next, $T_2 = C_4C_3 - C_2$. Since C_4, C_3, C_2 are sums of positive parameter products, T_2 becomes a sum of positive higher order products, and hence $T_2 > 0$. Finally, $T_4 = C_1(C_2C_3C_4 - C_1C_4^2 - C_2^2) - C_0(C_3^2C_4 - C_2C_3 - 2C_1C_4 + C_0)$. Because all $C_i > 0$ when $\mathcal{R}_0 < 1$, each bracketed term is a positive combination of parameter products. Therefore $T_4 > 0$. Hence all even Hurwitz determinants are positive.

By the Routh–Hurwitz criterion, all eigenvalues have negative real parts whenever $\mathcal{R}_0 < 1$. Therefore, the disease-free equilibrium E_0 is locally asymptotically stable.

If $\mathcal{R}_0 > 1$, then

$$k_7 > k_4 k_5^2 k_6.$$

Thus $C_1 < 0$ and $C_0 < 0$, while the higher order coefficients remain positive. The sequence $C_5, C_4, C_3, C_2, C_1, C_0$ has exactly one sign change. By Descartes' Rule of Signs, the characteristic equation possesses exactly one positive real root. Hence at least one eigenvalue has positive real part.

Therefore, the disease-free equilibrium E_0 is unstable whenever $\mathcal{R}_0 > 1$. □

Observation 7 *The basic reproduction number of the model is given by*

$$\mathcal{R}_0 = \sqrt{\frac{\sigma_W \sigma_V \beta_W \beta_V b_V^2}{(\sigma_W + \mu_W)(\gamma_W + \mu_W)^2(\sigma_V + \mu_V)}}.$$

The condition $\mathcal{R}_0 < 1$ implies the following biological relationships:

(i) The infection dies out when the combined transmission rates between humans and vectors are sufficiently small compared to the recovery and natural death rates in the population.

(ii) If the human recovery rate is sufficiently high relative to the transmission rates, the infection cannot persist and the disease-free equilibrium remains stable.

(iii) Effective reduction of vector survival or progression rates through control measures decreases the ability of the vector population to sustain transmission.

(iv) Lower vertical transmission probability significantly reduces the overall reproduction potential of the disease.

(v) Increased natural mortality in either human or vector populations shortens the infectious period and reduces the possibility of sustained disease spread.

Hence, the disease-free equilibrium is locally asymptotically stable whenever recovery and removal mechanisms dominate transmission processes in both human and vector populations.

6 Conclusion

In the present paper, we developed a graph-theoretic framework to study Zika virus transmission incorporating both vector-borne infection and vertical transmission from infected mothers to newborn babies. Adult humans, newborns, and vector populations were represented as distinct vertices of a weighted directed graph, allowing infection pathways, maturation processes, recovery, and mother-to-child transmission to be encoded directly within the adjacency matrix structure. Using the characteristic polynomial of the infection subgraph, an energy-based reproduction number was

introduced and defined as

$$R_0 = \mathcal{E}(D) + 2\mathcal{E}_c(D) = \sum_{k=1}^{n} |\mathrm{Re}(\lambda_k)| + 2\sum_{k=1}^{n} |\mathrm{Im}(\lambda_k)|,$$

where λ_k are the eigenvalues associated with the infected vertices of the adjacency matrix. Unlike classical next-generation approaches, this formulation captures transmission energy flow through vertical (adult–newborn) edges and vector-mediated cycles simultaneously. The resulting reproduction threshold quantifies the combined contribution of adult-to-newborn transmission, maturation transitions, and mosquito-driven infection loops. The numerical analysis of the reproduction number shows that transmission-related parameters exert the strongest positive influence on epidemic growth.

To assess the dynamics near the disease-free state, the disease-free equilibrium (DFE) was obtained by setting all infected adult, newborn, and vector compartments equal to zero while maintaining susceptible classes at steady-state levels. The Jacobian matrix evaluated at the DFE was analyzed using the Routh–Hurwitz stability criteria together with Gershgorin's circle theorem. The classical basic reproduction number at the DFE is given by

$$\mathcal{R}_0 = \sqrt{\frac{\sigma_W \sigma_V \beta_W \beta_V b_V^2}{(\sigma_W + \mu_W)(\gamma_W + \mu_W)^2(\sigma_V + \mu_V)}}.$$

The DFE is locally asymptotically stable whenever $\mathcal{R}_0 < 1$ and becomes unstable when $\mathcal{R}_0 > 1$. The stability of the disease-free equilibrium depends on the balance between transmission parameters (β_W, β_V, b_V) and removal parameters (γ_W, μ_W, μ_V). Increasing recovery or natural mortality reduces the spectral radius and drives $\mathcal{R}_0$ below unity. Although vector transmission dominates the primary infection cycle, vertical transmission amplifies persistence by sustaining infection within the newborn compartment, thereby increasing the overall reproduction potential of the system.

Future research may extend this framework to incorporate vaccination, optimal control, stochastic effects, and spatial heterogeneity within the weighted adjacency matrix. The matrix structure itself can be modified and reanalyzed under alternative spectral energy measures or different eigenvalue-based thresholds. Moreover, the same graph-theoretic approach can be adapted to investigate other vertically transmitted or vector-borne viral diseases by redefining vertices and transmission weights accordingly.

References

[1] Ferguson, N. M., Cucunubá, Z. M., Dorigatti, I., Nedjati-Gilani, G. L., Donnelly, C. A., Basáñez, M., Nouvellet, P., & Lessler, J. (2016). Countering the Zika epidemic in Latin America. Science, 353(6297), 353–354. https://doi.org/10.1126/science.aag0219

[2] Suparit, P., Wiratsudakul, A., & Modchang, C. (2018). A mathematical model for Zika virus transmission dynamics with a time-dependent mosquito biting rate.

Theoretical Biology and Medical Modelling, 15(1), 11. https://doi.org/10.1186/s12976-018-0083-z

[3] Barve, T., Tiwari, S. K., & Porwal, P. (2022). A mathematical model for the sexual transmission of Zika virus based on gender and symptoms. South East Asian J of Mathematics and Mathematical Sciences, 18(02), 87–98. https://doi.org/10.56827/seajmms.2022.1802.9

[4] Banuelos, S., Martinez, M., Mitchell, C., & Prieto-Langarica, A. (2019). Using mathematical modelling to investigate the effect of the sexual behaviour of asymptomatic individuals and vector control measures on Zika. Letters in Biomathematics, 6(1). https://doi.org/10.30707/lib6.1banuelos

[5] Agusto, F., Bewick, S., & Fagan, W. (2017). Mathematical model of Zika virus with vertical transmission. Infectious Disease Modelling, 2(2), 244–267. https://doi.org/10.1016/j.idm.2017.05.003

[6] Chitnis, N. (2005). Deterministic and stochastic models of malaria transmission. Ph.D. Thesis, University of Arizona, Tucson.

[7] Chartrand, G., & Zhang, P. (2005). Introduction to graph Theory. McGraw-Hill Science, Engineering & Mathematics.

[8] Renisa, P., Sujitha, S., & Angel Jebitha, M. K. (2025). A new approach to modelling of Zika virus dissemination by vector using graph theory. *Discontinuity, Nonlinearity, and Complexity* (Communicated).

[9] Gutman, I. (1978). The energy of a graph. Berichte der Mathematisch-Statistischen Sektion im Forschungszentrum Graz, 103, 1–22.

[10] Bhat, M. A. (2017). Energy of weighted digraphs. Discrete Applied Mathematics, 223, 1–14. https://doi.org/10.1016/j.dam.2017.01.034

[11] Khan, M., Farooq, R., & Rada, J. (2017). Complex adjacency matrix and energy of digraphs. Linear and Multilinear Algebra, 65, 2170 - 2186. https://doi.org/10.1080/03081087.2016.1265064

[12] Hafeez, S., & Khan, M. (2018). Iota energy of weighted digraphs. Transactions on Combinatorics, 7(3), 55–73. https://doi.org/10.22108/toc.2018.109248.1546

[13] Heffernan, J. M., Smith, R. J., & Wahl, L. M. (2005). Perspectives on the basic reproductive ratio. Journal of the Royal Society, Interface, 2(4), 281–293. https://doi.org/10.1098/rsif.2005.0042

[14] Hethcote, H. W. (2000). The mathematics of infectious diseases. SIAM Review, 42(4), 599–653. https://doi.org/10.1137/S0036144500371907